A Non-Iterative Technique for Phase Noise ICI Mitigation in Packet-Based OFDM Systems

Payam Rabiei, *Student Member IEEE*, Won Namgoong *Senior Member IEEE*,

and Naofal Al-Dhahir, *Fellow IEEE*,

Abstract

In this paper, a practical approach for detecting packet-based orthogonal frequency division multiplexing (OFDM) signals in the presence of phase noise is presented. An OFDM packet consists of several OFDM symbols with full-pilot symbols at the beginning followed by consecutive data symbols. Based on the full-pilot OFDM symbol, a frequency-domain joint phase noise and channel vector estimator is first derived. It is shown that the phase noise vector can be estimated by maximizing a constrained quadratic form without requiring knowledge of the channel vector. This estimated phase noise vector is then used to compute the least squares channel estimator. Assuming that the channel is constant during each packet, the estimated channel is used in subsequent data OFDM symbols for equalization and data detection. Since phase noise changes from one OFDM symbol to the next, the scattered pilots in each data OFDM symbol are used to *non-iteratively* estimate and mitigate the phase noise induced interference. A significant improvement in the signal-to-interference-plus-noise ratio is achieved using our proposed algorithms.

This work was supported in part by the National Science Foundation (NSF) under contract CCF 07-33124 and by a gift from Research In Motion (RIM) Inc.

Index Terms

OFDM, phase noise, channel estimation, linear interpolation, scattered pilots.

I. Introduction

HIGH-rate multi-carrier transmission schemes are attractive in modern communication systems, which require broadband data transmission with high spectral efficiency. However, the sensitivity of a coherent receiver to the local oscillator (LO) phase noise increases for large signal constellation sizes. This issue becomes more pronounced for orthogonal frequency division multiplexing (OFDM) systems [1] since the transmission bandwidth is divided into narrower sub-channels. Moreover, as the carrier frequency increases, the phase noise effects become more significant, potentially limiting the overall system performance. Phase noise manifests itself in two ways [2], [3] - a common phase error (CPE), which is an identical phase rotation in all sub-carriers, and inter-carrier interference (ICI), which is a result of the loss of orthogonality among sub-carriers.

A. Previous Work

The effect of phase noise on the performance of OFDM systems has been extensively analyzed (see e.g. [2], [4]–[6]) using the conventional approach of estimating the CPE term only. Since correcting for CPE yields poor detection performance in the presence of large phase noise, estimation and compensation of ICI caused by phase noise were considered in [3], [7]–[9]. As ICI mitigation involves de-convolving the phase noise spectral components from unknown data sub-carriers, the authors of [7]–[9] use an iterative algorithm for joint data and phase noise estimation. Specifically, CPE is estimated using scattered pilots and the data symbols are detected using the estimated CPE, after which phase noise is re-estimated using the detected data. A common problem with iterative schemes is that they suffer from error propagation if iteration is performed on the uncoded data, or from long latency and high complexity if iteration is performed after the Viterbi decoder [3]. Long latency is not practical in many packet-based systems that require fast packet acknowledgement, such as 802.11a/n. Moreover, perfect knowledge of the channel was assumed in [2], [3] during the full-pilot OFDM symbol transmission. An approach based on joint time-domain channel and phase noise estimation was investigated in [10] which requires an $N \times N$ matrix inversion where N is the discrete Fourier transform (DFT) size.

B. Our Contributions

In this paper, we propose a practical approach to detect packet-based OFDM signals in the presence of phase noise. An OFDM packet consists of several consecutive OFDM symbols with few full-pilot symbols at the beginning which are typically used for channel estimation, followed by data symbols in which data and pilot subcarriers are multiplexed together. We design efficient schemes for both channel estimation during the full-pilot OFDM symbol and data detection in subsequent data OFDM symbols with scattered pilots. In our proposed scheme, the full-pilot OFDM symbol is used to jointly estimate the channel and phase noise vectors. We propose a novel frequency-domain estimator in contrast to [10] which follows a time-domain approach. The motivation to perform the estimation in the frequency domain is the fact that the phase noise process can be well approximated by a few frequency spectral components [4] and this property can be used to reduce the complexity of the proposed estimation algorithm significantly.

For indoor systems such as wireless local area networks (WLAN), the channel is constant during each OFDM packet (i.e. no mobility). However, phase noise changes from one OFDM symbol to the next [3]. We propose to use the *scattered pilots* in each data OFDM symbol to estimate the spectral components of the phase noise process in the same OFDM symbol. Specifically, a *non-iterative* approach to mitigate ICI in data OFDM symbols is investigated where the CPE terms of at least two consecutive data OFDM symbols are estimated using their own scattered pilots. Next, the phases of the estimated CPEs are set as the phases corresponding to the middle samples of each time-domain OFDM symbol (see Fig. 5, 6). Interpolation between the phases of these two points provides an estimate of the phase transition from the middle sample of the first OFDM symbol to the next. The interpolator is derived by minimizing the mean squared error (MSE) with respect to the actual underlying phase noise process as the cost function. We prove that, for small phase noise, a straight line connecting the phases of the two middle points minimizes the MSE.

Our proposed approach achieves significant performance improvement compared to conventional OFDM receivers with single tap per sub-carrier frequency-domain equalizers. Based on the full-pilot OFDM symbol, our joint channel and phase noise estimator provides an accurate channel estimate in the presence of phase noise. For data OFDM symbols, linear phase interpolation of CPE mitigates a considerable amount of ICI. Furthermore, no iterations are employed in the estimation process neither during the full-pilot OFDM transmission stage nor during the data OFDM detection stage.

The rest of the paper is organized as follows. In Section II, the system model is described and the joint frequency-domain channel and phase noise estimator is derived. In Section III, phase noise estimation and tracking is described. In Section IV, the effective signal to noise plus interference ratio (SINR) is analyzed and the improvement due to our proposed algorithm is quantified. Simulation results are given in Section V and the paper is concluded in Section VI.

II. System Model and Joint Estimator

A. System Model and Notation

The notation of this paper is as follows. All vectors and matrices in the time-domain are represented by $\bar{a}$ and $\bar{A}$, respectively, while those in the frequency-domain are represented by $\boldsymbol{a}$ and $\boldsymbol{A}$, respectively. Unless otherwise stated, all vectors are assumed to be column vectors. The nth element of vector $\bar{a}$ is denoted by $\bar{a}_n$ and the mth vector within a set of similar vectors is denoted by $\bar{a}^m$. Also, the (m, n)th element of the matrix $\boldsymbol{A}$ is denoted by $\boldsymbol{A}(m, n)$. Furthermore, $\bar{a}^{mT}$ and $\bar{a}^{mH}$ are the transpose and Hermitian transpose of $\bar{a}^m$ respectively. a^* is the complex conjugate of the scalar a. The estimate of a vector $\boldsymbol{a}^m$ is denoted by $\widehat{\boldsymbol{a}}^m$.

In many packet-based OFDM systems, carrier frequency offset (CFO) synchronization and timing synchronization are performed based on repetitive time-domain training sequences [11], [12], [13]. In this work, we assume that the CFO and timing offset synchronization have been determined and compensated for, based on these repetitive training sequences. Channel estimation is performed based on full-pilot OFDM symbol following the repetitive training sequences. One full-pilot OFDM symbol with superscript of zero (i.e. $m = 0$) is assumed in this paper. If $m \neq 0$, that OFDM symbol is a data symbol. Since the channel is assumed constant within the packet (i.e. no mobility), the superscript is omitted for the channel vectors and matrices for simplicity of notation.

The signal model in the presence of phase noise is studied in [2], [14]. At the nth signal sample of the mth OFDM symbol, phase noise introduces a random phase rotation of $e^{j\bar{\phi}_n^m}$ in the time-domain where $\bar{\phi}_n^m = \bar{\phi}_{n-1}^m + \varepsilon$ and $\varepsilon \sim \mathcal{N}(0, \sigma_\varepsilon^2)$ [2] [3] [15]. The phase noise variance is $\sigma_\varepsilon^2 = 2\pi\beta T_s$ [16] [17], where T_s is the OFDM symbol time duration and β is the two-sided 3-dB bandwidth of the phase noise process. This effect can be expressed as convolution[1] in the frequency-domain and the received signal $\boldsymbol{r}_k^m$ can be written as

$$\boldsymbol{r}_k^m = \sum_{q=0}^{N-1} \boldsymbol{x}_q^m \boldsymbol{h}_q \boldsymbol{p}_{\langle k-q \rangle}^m + \boldsymbol{w}_k^m \quad : \quad 0 \leq k \leq N-1 \tag{1}$$

where N is the OFDM symbol size, $\boldsymbol{x}_q^m$ for $m=0$ is the qth pilot sample of the pilot vector $\boldsymbol{x}^0 = [\boldsymbol{x}_0^0 \cdots \boldsymbol{x}_{N-1}^0]^T$, $\boldsymbol{h}_q$ is the qth element of the channel vector $\boldsymbol{h} = [\boldsymbol{h}_0 \cdots \boldsymbol{h}_{N-1}]^T$ and $\boldsymbol{p}_q^m$ is the qth spectral component of the phase noise vector $\boldsymbol{p}^m = [\boldsymbol{p}_0^m \cdots \boldsymbol{p}_{N-1}^m]$, respectively. Note that $\boldsymbol{p}^m$ is defined as a row vector. The notation $\langle \cdot \rangle$ denotes the modulo-N operation. Vector $\boldsymbol{x}^0$ consists of pilot tones which are known to the receiver. This vector is referred to as the full-pilot OFDM symbol. $\boldsymbol{w}^m$ is additive complex noise Gaussian distributed with zero mean and variance $\sigma_{\boldsymbol{w}}^2$. The kth phase noise spectral component of the mth OFDM symbol $\boldsymbol{p}_k^m$, can be written as [3]

$$\boldsymbol{p}_k^m = \frac{1}{N} \sum_{n=0}^{N-1} e^{j\bar{\phi}_n^m} \exp\left(\frac{-j2\pi nk}{N}\right) \ : \ 0 \leq k \leq N-1 \tag{2}$$

The channel response at the kth frequency sub-carrier is given by

$$\boldsymbol{h}_k = \frac{1}{\sqrt{N}} \sum_{l=0}^{L-1} \bar{h}_l \exp\left(\frac{-j2\pi kl}{N}\right) \ : \ 0 \leq k \leq N-1 \tag{3}$$

where $\bar{h}_l$ is the lth tap of the time-domain channel impulse response of length L, which is assumed to be less than the length of the cyclic prefix to maintain orthogonality among the sub-carriers in each OFDM symbol. The channel taps are assumed to be uncorrelated zero-mean complex Gaussian random variables with an exponential power delay profile and variance $\mathsf{E}[|\bar{h}|^2] = \sigma_h^2$, where $\mathsf{E}[\cdot]$ is the statistical expectation operation.

[1]Modulo-N circular convolution because of the cyclic prefix appended at the end of each OFDM symbol.

B. Channel Estimation

Assuming that the pilot tones are drawn from a constant-modulus signal constellation, i.e. $\boldsymbol{x}_q^0 \boldsymbol{x}_q^{0*} = \mathcal{E}_{\boldsymbol{x}}$, the least squares (LS) estimator of the time-domain channel vector $\bar{h} = [\bar{h}_0 \cdots \bar{h}_{L-1}]^T$ which collects the channel taps in the time-domain can be written as [18]

$$\hat{\bar{h}} = \arg\min_{\bar{h}} \left[-\log f(\boldsymbol{r}^0 | \boldsymbol{p}^{0T}, \bar{h}) \right] \tag{4}$$

where $f(\cdot)$ is the conditional probability density function (PDF) of the received vector, $\boldsymbol{r}^0$, given the phase noise and the channel vectors. Note that Baysian estimation is not considered in this paper which means no apriori knowledge of $f(\bar{h})$ and $f(\boldsymbol{p}^{0T})$ is available at the receiver. Re-writing (1) in compact matrix notation, we have $\boldsymbol{r}^0 = \boldsymbol{P}^0 \boldsymbol{X}^0 \boldsymbol{D} \bar{h} + \boldsymbol{w}^0$, where $\boldsymbol{D}$ is the $N \times L$ DFT matrix with $\boldsymbol{D}(n,l) = \frac{1}{\sqrt{N}} \exp\left(-j2\pi nl/N\right)$, $\boldsymbol{X}^0$ is a diagonal matrix of pilot tones, $\boldsymbol{P}^0$ is a column-wise circulant matrix whose first column is $\boldsymbol{p}^{0T}$ and the following columns are cyclically-shifted versions of it. The conditional PDF in (4) is Gaussian [18] i.e. $f(\boldsymbol{r}^0|\boldsymbol{p}^{0T}, \bar{h}) = \alpha \exp(-\|\boldsymbol{r}^0 - \boldsymbol{P}^0 \boldsymbol{X}^0 \boldsymbol{D} \bar{h}\|^2/\sigma_{\boldsymbol{w}}^2)$ where α is a constant and the LS channel estimate is derived by minimizing its exponent

$$\begin{aligned} \hat{\bar{h}} &= \arg\min_{\bar{h}} \left\| \boldsymbol{r}^0 - \boldsymbol{P}^0 \boldsymbol{X}^0 \boldsymbol{D} \bar{h} \right\|^2 \\ &= \frac{1}{\mathcal{E}_{\boldsymbol{x}}} \boldsymbol{D}^H \boldsymbol{X}^{0H} \boldsymbol{P}^{0H} \boldsymbol{r}^0 \end{aligned} \tag{5}$$

The second line in (5) is derived by differentiating the squared norm with respect to $\bar{h}^H$ and setting it to zero. Note that it can be easily shown from (2) that $\boldsymbol{P}^0$ is an orthonormal matrix i.e. $\boldsymbol{P}^0 \boldsymbol{P}^{0H} = \boldsymbol{I}$ where $\boldsymbol{I}$ is the identity matrix. This fact has been used in derivation of the LS channel estimate in (5). This channel estimate is a function of the unknown phase noise matrix $\boldsymbol{P}^0$ and, therefore, it can not be computed until $\boldsymbol{P}^0$ is estimated beforehand. Phase noise estimation is described in the next subsection.

C. Phase Noise Estimation

The dependence of the cost function in (4) on the channel vector can be removed by substituting its LS estimate from (5) as follows

$$
\begin{aligned}
\widehat{\boldsymbol{p}}^{0T} &= \arg\min_{\boldsymbol{p}^{0T}}[-\log f(\boldsymbol{r}^0|\boldsymbol{p}^{0T},\widehat{\bar{h}})] \\
&= \arg\min_{\boldsymbol{p}^{0T}} \|\boldsymbol{r}^0 - \frac{1}{\mathcal{E}_{\boldsymbol{x}}}\boldsymbol{P}^0\boldsymbol{X}^0\boldsymbol{D}\boldsymbol{D}^H\boldsymbol{X}^{0H}\boldsymbol{P}^{0H}\boldsymbol{r}^0\|^2 \\
&= \arg\min_{\boldsymbol{p}^{0T}}[\boldsymbol{r}^{0H}\boldsymbol{r}^0 - \frac{1}{\mathcal{E}_{\boldsymbol{x}}}\boldsymbol{r}^{0H}\boldsymbol{P}^0\boldsymbol{X}^0\boldsymbol{D}\boldsymbol{D}^H\boldsymbol{X}^{0H}\boldsymbol{P}^{0H}\boldsymbol{r}^0] \\
&= \arg\min_{\boldsymbol{p}^{0T}}[\boldsymbol{r}^{0H}\boldsymbol{r}^0 - \frac{1}{\mathcal{E}_{\boldsymbol{x}}}\boldsymbol{r}^{0H}\boldsymbol{P}^0\boldsymbol{X}^0 \\
&\qquad\qquad \times(\boldsymbol{I}-\boldsymbol{B}\boldsymbol{B}^H)\boldsymbol{X}^{0H}\boldsymbol{P}^{0H}\boldsymbol{r}^0] \\
&= \arg\max_{\boldsymbol{p}^{0T}} \boldsymbol{r}^{0H}\boldsymbol{P}^0\boldsymbol{X}^0\boldsymbol{B}\boldsymbol{B}^H\boldsymbol{X}^{0H}\boldsymbol{P}^{0H}\boldsymbol{r}^0 \\
&= \arg\max_{\boldsymbol{p}^{0T}} \boldsymbol{p}^0\boldsymbol{R}^{0H}\boldsymbol{X}^0\boldsymbol{B}\boldsymbol{B}^H\boldsymbol{X}^{0H}\boldsymbol{R}^0\boldsymbol{p}^{0H} \\
&= \arg\max_{\boldsymbol{p}^{0T}} \boldsymbol{p}^0\boldsymbol{M}\boldsymbol{p}^{0H}
\end{aligned} \tag{6}
$$

where $\boldsymbol{M} \triangleq \boldsymbol{R}^{0H}\boldsymbol{X}^0\boldsymbol{B}\boldsymbol{B}^H\boldsymbol{X}^{0H}\boldsymbol{R}^0$. In the definition of $\boldsymbol{M}$, $\boldsymbol{B}$ is an $N \times (N-L)$ matrix consisting of the last $(N-L)$ columns of the full $N \times N$ DFT matrix and, therefore, concatenating $\boldsymbol{B}$ with $\boldsymbol{D}$ constructs a full $N \times N$ DFT matrix. $\boldsymbol{R}^0$ is a circulant matrix built from the received signal vector $\boldsymbol{r}^0$.

Our objective is to solve the resulting quadratic form in (6) subject to the constraint that *all* time-domain phase noise elements are small and lie in the unit circle, i.e. they are *all* in the form of $e^{j\bar{\phi}_n^0} \approx 1 + j\bar{\phi}_n^0$. Using (2) to transform this constraint to the frequency-domain, for $k = 0$ we get

$$
\boldsymbol{p}_0^0 = \frac{1}{N}\sum_{n=0}^{N-1} e^{j\bar{\phi}_n^0} \approx \frac{1}{N}\sum_{n=0}^{N-1}(1+j\bar{\phi}_n^0) = 1 + j\frac{1}{N}\sum_{n=0}^{N-1}\bar{\phi}_n^0 \tag{7}
$$

Therefore, a proper constraint in the frequency-domain is that the real part of $\boldsymbol{p}_0^0$ is 1[2]. This constraint follows directly from the small phase noise assumption in the time-domain.

Defining $\boldsymbol{e}$ as a $1 \times N$ row vector with first entry equal to one and zeros otherwise, we can formulate the proposed constraint as $\boldsymbol{e} \times \Re(\boldsymbol{p}^0)^T = 1$, where $\Re(\boldsymbol{p}^0)$ is the real part of $\boldsymbol{p}^0$. Therefore, the constrained cost function is given by

$$J = \boldsymbol{p}^0 \boldsymbol{M} \boldsymbol{p}^{0H} - \lambda \left(\boldsymbol{e} \times \Re(\boldsymbol{p}^0)^T - 1 \right) \tag{8}$$

where λ is a constant Lagrange multiplier.

Proposition 2.1: The solution to the constrained cost function in (8) is given by

$$\begin{aligned} \Im(\widehat{\boldsymbol{p}}^0)^T &= \lambda \boldsymbol{S} \boldsymbol{e}^T \\ \Re(\widehat{\boldsymbol{p}}^0)^T &= \lambda \boldsymbol{\Gamma}^{-1} (\boldsymbol{\Lambda}^T \boldsymbol{S} + \boldsymbol{I}) \boldsymbol{e}^T \end{aligned} \tag{9}$$

where $\boldsymbol{\Gamma}$ and $\boldsymbol{\Lambda}$ are the real and imaginary parts of the Hermitian matrix $\boldsymbol{M}$, respectively, $\Im(\widehat{\boldsymbol{p}}^0)$ is the imaginary part of $\widehat{\boldsymbol{p}}^0$ and $\boldsymbol{S} \triangleq \left[\boldsymbol{I} + \left(\boldsymbol{\Gamma}^{-1} \boldsymbol{\Lambda} \right)^2 \right]^{-1} \boldsymbol{\Gamma}^{-1} \boldsymbol{\Lambda} \boldsymbol{\Gamma}^{-1}$. The Lagrange multiplier can be found by satisfying the constraint $\boldsymbol{e} \times \Re(\boldsymbol{p}^0)^T = 1$ which gives

$$\lambda = \frac{1}{\boldsymbol{e}[\boldsymbol{\Gamma}^{-1} \boldsymbol{\Lambda}^T \boldsymbol{S} + \boldsymbol{\Gamma}^{-1}] \boldsymbol{e}^T} \tag{10}$$

Proof: See Appendix I. ■

The complexity of the above estimator can be reduced by considering only the most significant elements of $\boldsymbol{p}^0$. Based on the analysis in [4], the phase noise process can be modeled as a low-pass process and, therefore, the row vector $\boldsymbol{p}^m$ can be well approximated by estimating its $Q+1$ elements only, i.e. $\boldsymbol{p}_{N-Q/2}^m, \cdots, \boldsymbol{p}_{N-1}^m, \boldsymbol{p}_0^m, \cdots, \boldsymbol{p}_{Q/2}^m$. As a result, all the matrices in the estimator of (9) can be reduced in size accordingly. The remaining

[2]Since this constraint is approximate, the estimated phase noise vector is biased. This bias does not cause any performance loss since it will be averaged out during data transmission stage.

phase noise spectral components are set to zero, since they are in fact very small quantities. Therefore, $\boldsymbol{P}^m$ has a circulant and approximately banded structure with the main diagonal equal to the CPE term and $Q/2$ elements above and below the main diagonal. After estimating the real and imaginary parts of the phase noise vector in the frequency domain, the circulant banded matrix $\widehat{\boldsymbol{P}}^0$ is constructed and substituted back into (5) for channel estimation. Note that the cost function in (8) is independent of the channel. As a result, no iterations are needed in the joint channel and phase noise estimation.

In summary, the joint estimation is performed in two steps. In the first step, $Q+1$ phase noise spectral elements are estimated using (9). In the second step, the estimated phase noise matrix is used in (5) to compute the LS channel estimate.

III. Data OFDM Phase Noise Estimation

The channel estimate computed during the full-pilot OFDM symbol is used for equalization and decoding of the data OFDM symbols. Unlike the channel response, which is assumed constant for the duration of a packet, the phase noise matrix $\boldsymbol{P}^m$ changes from one OFDM symbol to the next. Therefore, this matrix has to be estimated for each OFDM symbol to achieve acceptable bit error rate (BER) performance. The scattered pilots inserted in every data OFDM symbol are used to estimate $\boldsymbol{P}^m$ for $m > 0$.

To mitigate ICI using these scattered pilots, we propose a non-iterative interpolation-based technique to track the random phase variations across the time-domain data samples in a given OFDM symbol. Our proposed approach differs from all existing approaches in the literature [3], [7]–[9] which perform joint *iterative* data and phase noise detection as explained in the introduction section. We propose two phase interpolation schemes depending on whether the receiver is able to buffer one OFDM symbol or not. In the first scheme, interpolation is performed between the estimated CPE associated with the current data OFDM symbol and the estimated CPE of the previous data OFDM symbol. Therefore, the receiver does not suffer from any latency or buffering requirements.

In the second scheme, interpolation is performed based on the estimated CPEs of the current, the previous, and the next OFDM symbols. Therefore, the actual detection of the mth received OFDM symbol takes place after reception of the $(m+1)$th OFDM symbol. Although the performance of the second scheme is superior to the first scheme, its drawback is the need for one OFDM symbol buffer and a latency of one OFDM symbol.

A. Interpolation Between Consecutive OFDM Symbols

Phase interpolation is performed between the CPE estimates of two consecutive OFDM symbols. In the data OFDM symbol, we have from (1) that

$$\boldsymbol{r}_k^m = \boldsymbol{p}_0^m \boldsymbol{x}_k^m \boldsymbol{h}_k + \sum_{q=0, q\neq k}^{N-1} \boldsymbol{x}_q^m \boldsymbol{h}_q \boldsymbol{p}_{\langle k-q \rangle}^m + \boldsymbol{w}_k^m \ : \ m \neq 0 \tag{11}$$

where the second term in (11) can be viewed as interference because of the unknown data. The CPE estimate is given by [2], [7]

$$\widehat{\boldsymbol{p}}_0^m = \frac{\sum_k \boldsymbol{r}_k^m \widehat{\boldsymbol{h}}_k^* \boldsymbol{x}_k^{m*}}{\sum_k \mathcal{E}_{\boldsymbol{x}} |\widehat{\boldsymbol{h}}_k|^2} \quad k \in \text{pilots} \tag{12}$$

Assuming that the cyclic prefix length is C, the estimated CPEs of the first and the second[3] data OFDM symbols are interpolated into $N+C$ intermediate points by designing a filter $\bar{G}$, which minimizes the MSE between the actual phase noise process and the phase-interpolating function. This can be written as

$$\bar{G}_{\text{opt}} = \arg\min_{\bar{G}} \mathsf{E}\left[\left|\bar{\theta} - \bar{G}\boldsymbol{u}\right|^2\right] = \boldsymbol{\Phi}_{\theta\boldsymbol{u}} \boldsymbol{\Phi}_{\boldsymbol{u}\boldsymbol{u}}^{-1} \tag{13}$$

[3]The interpolation is performed between the first and the second data OFDM symbols for simplicity of notation and there is no loss of generality incurred. The procedure can be easily generalized to the mth and $(m+1)$th data OFDM symbols.

where $\boldsymbol{u} = [\widehat{\boldsymbol{p}}_0^1 \;\; \widehat{\boldsymbol{p}}_0^2]^T$ and $\bar{\theta} = [e^{j\bar{\phi}^1_{N/2}} \cdots e^{j\bar{\phi}^2_{N/2}}]^T$ is the actual time-domain phase noise vector which extends from the middle point of the first data OFDM symbol to the middle point of the second OFDM symbol. Therefore, the interpolation region starts from the sample index $N/2$ and ends at the sample index $3N/2 + C$ (see Figures 5 and 6). $\boldsymbol{\Phi}_{\theta \boldsymbol{u}}$ is the cross correlation matrix between $\bar{\theta}$ and $\boldsymbol{u}$, $\boldsymbol{\Phi}_{\boldsymbol{u}\boldsymbol{u}}$ is the autocorrelation matrix of $\boldsymbol{u}$ and $\bar{G}$ is an $(N + C) \times 2$ interpolator matrix with the optimum solution $\bar{G}_{\text{opt}}$, given in (13).

For a simpler solution, we propose to connect the two estimated CPE points using linear interpolator, $\bar{G}_L$, and we prove that for small phase noise levels, $\bar{G}_{\text{opt}}$ reduces to $\bar{G}_L$. The linearly approximated phase noise can be written as

$$\underbrace{\bar{\theta}_L}_{(N+C)\times 1} = \underbrace{\bar{G}_L}_{(N+C)\times 2} \boldsymbol{u} \tag{14}$$

where the nth row of $\bar{G}_L$ is given by

$$\bar{G}_L(n, :) = \frac{1}{N + C} [3N/2 + C - n \quad n - N/2] \tag{15}$$

for $N/2 \leq n < 3N/2 + C$.

Proposition 3.1: The optimum interpolation matrix $\bar{G}_{\text{opt}}$ between the first and the second data OFDM symbols reduces to the linear interpolation matrix $\bar{G}_L$ given in (14) if $\beta T_s \ll 1$.

Proof: See Appendix I. ■

B. Phase Noise Tracking Strategy

The receiver with no buffer (RNB) estimates the CPE of the second received OFDM symbol and links it to the CPE of the first symbol using matrix $\bar{G}_L$. Since $\bar{G}_L$ covers only the first half of the second symbol, the CPE is used for the samples of the second half (see Figure 5).

Further performance improvement can be achieved if the receiver has access to memory that allows buffering of one data OFDM symbol. The receiver with buffer (RWB) waits for the third OFDM symbol before detecting the second OFDM symbol (see Figure 6). Hence, RWB constructs the phase noise matrix of the second OFDM symbol, only after receiving the third data OFDM symbol.

As an example, assuming transmission of three consecutive OFDM data symbols, the estimated CPE points are assigned to samples $N/2$, $3N/2 + C$ and $5N/2 + 2C$. The region between the first and last CPE points (i.e., $N/2 \leq n < 5N/2 + 2C$) is defined as the interpolation region (see Figure 6). The major advantage of the RNB and RWB schemes is their low implementation complexity. There is a significant SINR improvement by performing the linear phase noise interpolation which will be confirmed by computer simulations in Section V.

C. Data Detection

After the phase noise process is linearly approximated by either RNB or RWB, the data symbol estimates are computed as follows

$$\widehat{\boldsymbol{x}}_k^m = \frac{\sum\limits_{q=-Q/2}^{Q/2} \widehat{\boldsymbol{p}}_{\langle q \rangle}^{m*} \boldsymbol{r}_{\langle k-q \rangle}^m}{\widehat{\boldsymbol{h}}_k} \tag{16}$$

where $k \in$ data sub-carriers and $m \neq 0$. Basically, instead of de-rotating each OFDM sample in the time domain, the receiver simply convolves the received signal by the estimated phase noise spectral components followed by a simple one-tap frequency-domain equalizer (FEQ). The convolution operation can be implemented as a matched-filter for the phase noise matrix since $\boldsymbol{P}^m$ is an orthogonal matrix. Note that the summation in (16) is only over $Q + 1$

elements and, therefore, it is very simple to implement. The soft output of the FEQ is passed to the Viterbi decoder or a hard decision is made based on $\widehat{\boldsymbol{x}}_k^m$. Both coded and uncoded bit error rate (BER) results are given in Section V.

IV. SINR ANALYSIS

In this section, we derive an expression for the minimum SINR improvement due to our proposed algorithms. Note that the overall SINR improvement is due to the channel estimator proposed in Section II together with linear phase noise interpolation in Section III. In the following analysis, we assume perfect channel knowledge for all cases and therefore, only the improvement due to linear interpolation is analyzed which is less than the maximum achievable SINR gain.

A. Conventional Receiver

In the conventional receiver, the channel is estimated during the full-pilot transmission by dividing the received signal by the pilot signal in the frequency-domain. In other words, the phase noise process is ignored at each sub-carrier since the receiver is unable to estimate and remove the effect of phase noise from the unknown channel response. Furthermore, data detection during data OFDM transmission is performed as if there is no phase noise. In this case, from (11) the SINR is given by

$$\gamma_{\text{conven}} \leq \frac{\mathsf{E}[|\widehat{\boldsymbol{p}}_0^m|^2]}{1-\mathsf{E}[|\widehat{\boldsymbol{p}}_0^m|^2]+\gamma^{-1}} \tag{17}$$

where $\gamma = \mathcal{E}_{\boldsymbol{x}}\sigma_{\boldsymbol{h}}^2/\sigma_{\boldsymbol{w}}^2$ is the matched-filter bound SNR. The right hand side of (17) is the maximum SINR which is achievable by ignoring the channel estimation error (i.e. perfect channel at the receiver). Using the derivations given in Appendix II, the SINR in (17) is given by

$$\gamma_{\text{conven}} \leq \frac{1 - \pi\beta N T_s/3}{\pi\beta N T_s/3 + \bar{\gamma}^{-1}} \mathrel{\mathring{=}} \frac{3}{\pi\beta N T_s} - 1 \tag{18}$$

where $\mathrel{\mathring{=}}$ denotes asymptotic equivalence as $\gamma \to \infty$.

B. Proposed Linear Phase Noise Interpolation Case

In this subsection, the effect of performing interpolation is studied and the SINR improvement is quantified compared to the conventional receiver. We assume that the receiver performs the proposed RWB phase noise interpolation of Section III during the data OFDM transmission. Assuming that the received signal in the data OFDM stage follows the model in (1), the receiver convolves this received vector with the estimated phase noise vector in the frequency-domain (which has already been computed using interpolation) to get

$$\begin{aligned} \boldsymbol{y}_k^m &= \sum_{q=-Q/2}^{Q/2} \widehat{\boldsymbol{p}}_{\langle q \rangle}^{m*} \boldsymbol{r}_{\langle k-q \rangle}^m \quad : \quad m \neq 0 \\ &= \boldsymbol{h}_k \boldsymbol{x}_k^m + \sum_{q=0}^{N-1} \boldsymbol{\eta}_{\langle k-q \rangle}^m \boldsymbol{h}_q \boldsymbol{x}_q^m + \sum_{q=0}^{N-1} \widehat{\boldsymbol{p}}_{\langle k-q \rangle}^{m*} \boldsymbol{w}_q^m \end{aligned} \tag{19}$$

$\boldsymbol{\eta}^m$ in (19) is the residual phase noise vector and the interference term in (19) is a result of phase noise estimation error. The receiver equalizes $\boldsymbol{y}_k^m$ by the estimated channel $\widehat{\boldsymbol{h}}_k$ in the frequency-domain to get the estimate of the transmitted information symbols. To simplify the analysis, the channel estimation error is ignored. Therefore, we have

$$\widehat{\boldsymbol{x}}_k^m = \frac{\boldsymbol{y}_k^m}{\boldsymbol{h}_k} = \boldsymbol{x}_k^m + \frac{\boldsymbol{i}_k^m}{\boldsymbol{h}_k} + \frac{\boldsymbol{w}_k^{\prime m}}{\boldsymbol{h}_k} \quad : \quad m \neq 0 \tag{20}$$

where $\boldsymbol{w}_k^{\prime m}$ is the equivalent noise which is still Gaussian with the same variance as $\boldsymbol{w}_k^m$ since the frequency-domain phase noise vector $\boldsymbol{p}^m$ is orthonormal and $\boldsymbol{i}_k^m$ is the interference which is the second term in (19). From (20), the maximum SINR can be derived as follows

$$\gamma_{\text{interpolation}} \leq \frac{1}{\displaystyle\sum_{q=0}^{N-1} \mathsf{E}\left[\left|\boldsymbol{\eta}_q^m\right|^2\right] + \gamma^{-1}} \tag{21}$$

The asymptotic SINR depends on the phase noise variance β, symbol period T_s, Q, N, the number of scattered pilots $|\mathcal{P}|$ and the cyclic prefix length C. As shown in Appendix III, the high-SNR asymptotic value of (21) can be derived to be

$$\gamma_{\text{interpolation}} \mathrel{\mathring{=}} \frac{9}{\left(1 + \dfrac{2}{|\mathcal{P}|} + \dfrac{C}{N}\right)\pi\beta N T_s} \tag{22}$$

Depending on the number of scattered pilots and the guard interval length, the asymptotic SINR expression in (22) provides improvement when compared to the expression in (18). For example, for $C = 16$, $N = 64$, $|\mathcal{P}| = 4$, $\beta = 1$kHz in an OFDM system with 20MHz bandwidth, the SINR improvement is 2.4dB. This improvement is solely due to the linear interpolation in data OFDM transmission stage and does not consider the effect of the phase noise resilient channel estimator during full-pilot OFDM transmission proposed in Section II-B. The simulation results show near 5dB overall improvement (see Figure 9).

V. NUMERICAL RESULTS

In this section, the performance of our proposed phase noise mitigation schemes is investigated. In our simulations, a packet is considered as one full-pilot OFDM symbol followed by three data OFDM symbols. The channel power delay profile is assumed exponential and the channel memory is assumed less than the cyclic prefix length to maintain sub-carrier orthogonality in each OFDM symbol.

Figure 2 shows the estimated phase noise process during one full-pilot OFDM symbol. The estimated frequency-domain phase noise vector $\widehat{\boldsymbol{p}}^0$ is assumed to have three elements denoted by $\widehat{\boldsymbol{p}}_0^0$, $\widehat{\boldsymbol{p}}_1^0$ and $\widehat{\boldsymbol{p}}_{N-1}^0$. This implies that Q is chosen to be two in our simulation. These three elements correspond to the three main diagonals of the circulant phase noise matrix $\widehat{\boldsymbol{P}}^0$ in the frequency domain.

The MSE of the channel estimate in the presence of phase noise is compared with the case when there is no phase noise in Figure 3. As it can be seen from the figure, the MSE of our proposed channel estimator is close to the scheme in [10]. In our scheme, only one super-diagonal and one sub-diagonal of $\boldsymbol{P}^0$ are estimated, i.e. $Q = 2$, while the entire time-domain phase noise vector of dimension N is estimated according to the algorithm in [10]. Also, compared to the channel estimation MSE in the conventional receiver, which ignores the phase noise during channel estimation stage, our proposed joint channel and phase noise scheme achieves significant performance improvement.

Figure 4 shows the channel estimation MSE as a function of Q for SNR of 30dB and different values of β. As it can be seen from the figure, if $Q = 0$ (i.e. only CPE is considered), the MSE is high. However, if we consider one sub- and one super-diagonal of $\boldsymbol{P}^m$ i.e. $Q = 2$, the MSE decreases significantly especially for high β. Moreover, as we further increase Q, little improvement in the channel estimation MSE is observed. This indicates that increasing Q to more than four results in negligible performance improvement and adds to the complexity of the estimation algorithm.

The RNB interpolation algorithm is illustrated in Figure 5 where the phase noise process is shown over two data OFDM symbols. The optimum interpolator together with its linear approximation connect the two CPEs of the consecutive data OFDM symbols. As it can be seen in this figure, CPE is used to cover the second half of the second data OFDM symbol. Note that in this case, the receiver has no knowledge about the CPE of the next data OFDM symbol. The RWB interpolation algorithm is also shown in Figure 6 over three data OFDM symbols. As it can be seen in the figure, $\boldsymbol{P}^m$ can be constructed only after reception of the $(m+1)$th data OFDM symbol.

Figure 7 illustrates the uncoded BER performance of the proposed channel and phase noise estimator. The packet structure described before is used with $Q = 2$ and the estimated channel is used to estimate phase noise and decode the data in the data transmission stage. The signal constellation is assumed to be 16-QAM with normalized energy; however, pilots are drawn from a BPSK constellation with the same average energy. The DFT size is 64 and the number of pilots is 4 which are equi-distant in each data OFDM symbol. From Figure 7, we observe that the performance of our proposed channel estimation method is better than the conventional method since there is an SINR improvement in estimating the channel. The BER performance is further improved by applying the RNB phase noise interpolation at the receiver. Further ICI mitigation is achieved by performing RWB interpolation, as seen in Figure 7. Moreover, the performance of the optimum interpolator is the same as the linear interpolator for $\beta = 1$kHz and a bandwidth of 20MHz.

The coded BER performance is shown in Figure 8. The coding rate is $1/2$ and the WLAN standard convolutional encoder $[133, 171]$ with the constraint length of 7 is used. The Viterbi decoder uses the soft information at the output of the detector in (16) with a decoding depth equal to five times the convolutional encoder constraint length. As it can be seen from Figure 8, our proposed algorithms result in significant performance improvements compared to the conventional receiver.

Figure 9 shows the SINR improvement (i.e. $\gamma_{\text{interpolation}}/\gamma_{\text{conven}}$) versus the matched-filter bound SNR $\gamma = \mathcal{E}_{\boldsymbol{x}}\sigma^2_{\boldsymbol{h}}/\sigma^2_{\boldsymbol{w}}$. The overall SINR improvement is approximately 5dB. The SINR improvement due to interpolation only is also plotted which shows good match to our analytical results in Section IV.

VI. Conclusion

In this paper, we proposed a low-complexity non-iterative frequency-domain joint channel and phase noise estimation algorithm for OFDM systems. The improved channel estimation algorithm in the presence of phase noise enhances the performance of data detection. Additional SINR improvement is achieved by performing phase noise interpolation during data OFDM transmission. Finally, we prove that the optimum interpolator (in the MMSE sense) is equivalent to the linear interpolator for small values of phase noise.

Appendix I

Proof of Proposition 2.1

Expanding $\boldsymbol{p}^0$ into its real and imaginary part, we can decompose the cost function as follows

$$\begin{aligned} J &= (\Re(\boldsymbol{p}^0) + j\Im(\boldsymbol{p}^0))\boldsymbol{M}(\Re(\boldsymbol{p}^0) - j\Im(\boldsymbol{p}^0))^T \\ &- \lambda(\boldsymbol{e} \times \Re(\boldsymbol{p}^0)^T - 1) \\ &= \Re(\boldsymbol{p}^0)\boldsymbol{\Gamma}\Re(\boldsymbol{p}^0)^T + \Im(\boldsymbol{p}^0)\boldsymbol{\Gamma}\Im(\boldsymbol{p}^0)^T + 2\Re(\boldsymbol{p}^0)\boldsymbol{\Lambda}\Im(\boldsymbol{p}^0)^T \\ &- \lambda(\boldsymbol{e}\Re(\boldsymbol{p}^0)^T - 1) \end{aligned} \tag{23}$$

Differentiating the cost function with respect to $\Re(\boldsymbol{p}^0)$ and $\Im(\boldsymbol{p}^0)$ and equating to zero we have

$$\begin{aligned} \frac{\partial J}{\partial \Re(\boldsymbol{p}^0)} &= \left[\boldsymbol{\Gamma}\Re(\boldsymbol{p}^0)^T + \boldsymbol{\Lambda}\Im(\boldsymbol{p}^0)^T\right] - \lambda \boldsymbol{e}^T = 0 \\ \frac{\partial J}{\partial \Im(\boldsymbol{p}^0)} &= \left[\boldsymbol{\Gamma}\Im(\boldsymbol{p}^0)^T - \boldsymbol{\Lambda}\Re(\boldsymbol{p}^0)^T\right] = 0 \end{aligned} \tag{24}$$

solving (24) jointly for the real and imaginary parts of phase noise vector we get

$$\begin{aligned}
\Re(\boldsymbol{p}^0)^T &= \boldsymbol{\Gamma}^{-1}\boldsymbol{\Lambda}^T\Im(\boldsymbol{p}^0)^T + \lambda\boldsymbol{\Gamma}^{-1}\boldsymbol{e}^T \\
\Im(\boldsymbol{p}^0)^T &= \boldsymbol{\Gamma}^{-1}\boldsymbol{\Lambda}\Re(\boldsymbol{p}^0)^T \\
&= \boldsymbol{\Gamma}^{-1}\boldsymbol{\Lambda}\left[\boldsymbol{\Gamma}^{-1}\boldsymbol{\Lambda}^T\Im(\boldsymbol{p}^0)^T + \lambda\boldsymbol{\Gamma}^{-1}\boldsymbol{e}^T\right] \\
&= \lambda\left[\boldsymbol{I} + \left(\boldsymbol{\Gamma}^{-1}\boldsymbol{\Lambda}\right)^2\right]^{-1}\boldsymbol{\Gamma}^{-1}\boldsymbol{\Lambda}\boldsymbol{\Gamma}^{-1}\boldsymbol{e}^T \\
&= \lambda\boldsymbol{S}\boldsymbol{e}^T
\end{aligned} \tag{25}$$

the Lagrange multiplier can be found by satisfying the constraint $\boldsymbol{e}\Re(\boldsymbol{p}^0)^T - 1$ which gives

$$\lambda = \frac{1}{\boldsymbol{e}\left[\boldsymbol{\Gamma}^{-1}\boldsymbol{\Lambda}^T\boldsymbol{S} + \boldsymbol{\Gamma}^{-1}\right]\boldsymbol{e}^T} \tag{26}$$

APPENDIX II

PROOF OF PROPOSITION 3.1

As mentioned in Section III-A without loss of generality and for simplicity of notation, the optimum interpolator between the CPE points of the first and second data OFDM symbols in a packet is derived. To prove the theorem, we need to evaluate the autocorrelation and the cross correlation matrices in (13). To find the autocorrelation matrix $\boldsymbol{\Phi}_{\boldsymbol{uu}}$, first note that

$$\begin{aligned}
\mathsf{E}\left[e^{j\Delta\phi}\right] &= \alpha^{-1}\int_{-\infty}^{\infty} e^{j\Delta\phi}\exp\left(-\frac{(\Delta\phi)^2}{2\sigma_\varepsilon^2|n-k|}\right)d\Delta\phi \\
&= \exp\left(-\frac{|n-k|\sigma_\varepsilon^2}{2}\right)
\end{aligned} \tag{27}$$

where $\alpha = \sqrt{2\pi\sigma_\varepsilon^2|n-k|}$, $\Delta\phi = \phi_n - \phi_k$. Using the result in (27) to compute the expected value of the CPE term, we get

$$\begin{aligned}
\mathsf{E}[\widehat{\boldsymbol{p}}_0^1\widehat{\boldsymbol{p}}_0^{1*}] &= \frac{1}{N^2}\sum_{n=0}^{N-1}\sum_{k=0}^{N-1}\mathsf{E}[e^{j\bar{\phi}_n^1}e^{-j\bar{\phi}_k^1}] \qquad (28)\\
&= \frac{1}{N^2}\sum_{n=0}^{N-1}\sum_{k=0}^{N-1}\exp(-\frac{|n-k|\sigma_\varepsilon^2}{2}) \\
&= \frac{2(1-\xi^{-N}) + N\xi^{-1} - N\xi}{N^2(1-\xi)(1-\xi^{-1})} = \mathsf{E}[\widehat{\boldsymbol{p}}_0^2\widehat{\boldsymbol{p}}_0^{2*}]
\end{aligned}$$

where $\xi = e^{\sigma_\varepsilon^2/2}$. For small phase noise, we can use the approximation $e^x \approx \sum_{i=0}^{2}(x^i/i!)$. Substituting these values in (28), we get $\mathsf{E}[\widehat{\boldsymbol{p}}_0^1\widehat{\boldsymbol{p}}_0^{1*}] = \mathsf{E}[\widehat{\boldsymbol{p}}_0^2\widehat{\boldsymbol{p}}_0^{2*}] \approx 1$. Similarly, we compute

$$\begin{aligned}\mathsf{E}[\widehat{\boldsymbol{p}}_0^1\widehat{\boldsymbol{p}}_0^{2*}] &= \frac{1}{N^2}\sum_{n=0}^{N-1}\sum_{k=N+C}^{(2N+C-1)}\mathsf{E}[e^{j\bar{\phi}_n^1}e^{-j\bar{\phi}_k^2}] \\ &= \frac{1}{N^2}\sum_{n=0}^{N-1}\sum_{k=N+C}^{(2N+C-1)}\exp(-\frac{|n-k|\sigma_\varepsilon^2}{2}) \\ &= \frac{(1-\xi^N)(\xi^{-(N+C)}-\xi^{-(2N+C)})}{N^2(1-\xi)(1-\xi^{-1})}\end{aligned} \tag{29}$$

Applying the approximations we used previously, we have $\mathsf{E}[\widehat{\boldsymbol{p}}_0^1\widehat{\boldsymbol{p}}_0^{2*}] = \mathsf{E}[\widehat{\boldsymbol{p}}_0^{1*}\widehat{\boldsymbol{p}}_0^2] \approx 1-\frac{\sigma_\varepsilon^2}{2}(N+C)$. Therefore, the inverse of the autocorrelation matrix $\boldsymbol{\Phi}_{\boldsymbol{uu}}$ can approximately be written as

$$\boldsymbol{\Phi}_{\boldsymbol{uu}}^{-1} \approx \frac{1}{(N+C)\sigma_\varepsilon^2}\begin{bmatrix} 1 & \frac{\sigma_\varepsilon^2}{2}(N+C)-1 \\ \frac{\sigma_\varepsilon^2}{2}(N+C)-1 & 1 \end{bmatrix} \tag{30}$$

Now, the cross-correlation matrix $\boldsymbol{\Phi}_{\theta\boldsymbol{u}}$ is an $(N+C)\times 2$ matrix which can be computed the same way as the entries of $\boldsymbol{\Phi}_{\boldsymbol{uu}}$ were calculated. However, since the vector $\bar{\theta}$ extends from the second-half of the first OFDM data symbol into the guard interval and then to the first-half of the second data symbol, i.e. the interpolation region defined in Section III-A, and depending on the index of the vector $\bar{\theta}$, we have two different expressions for the first column of $\boldsymbol{\Phi}_{\theta\boldsymbol{u}}$ as follows

$$\begin{aligned}\boldsymbol{\Phi}_{\theta\boldsymbol{u}}(n,1) = \mathsf{E}[\bar{\theta}_n^*\widehat{\boldsymbol{p}}_0^1] &= \frac{1}{N}\sum_{k=0}^{N-1}\exp(-\frac{|n-k|\sigma_\varepsilon^2}{2}) \\ &= \begin{cases}\dfrac{\xi^{-n}-1}{N(1-\xi)} + \dfrac{1-\xi^{n-N}}{N(1-\xi^{-1})} & : \ N/2 \le n < N \\ \dfrac{\xi^{-n}-\xi^{N-n}}{N(1-\xi)} & : \ N \le n < 3N/2 + C\end{cases}\end{aligned} \tag{31}$$

For both ranges of n, the two expressions in (31) converge to the same function using the Taylor expansion of ξ. Therefore, the first column of the cross-correlation matrix can be approximately written as

$$\mathbf{\Phi}_{\theta\boldsymbol{u}}(n,1) \approx 1 - \frac{\sigma_\varepsilon^2}{4}(2n-N) \quad : \quad N/2 \le n < 3N/2 + C \tag{32}$$

The second column of the cross-correlation matrix $\mathbf{\Phi}_{\theta\boldsymbol{u}}$, can be found in a similar way to be

$$\begin{aligned}\mathbf{\Phi}_{\theta\boldsymbol{u}}(n,2) &= \mathsf{E}[\bar{\theta}_n^* \widehat{\boldsymbol{p}}_0^2] = \frac{1}{N}\sum_{k=N+C}^{2N+C-1} \exp(-\frac{|n-k|\sigma_\varepsilon^2}{2}) \\ &= \begin{cases} \dfrac{\xi^{n-N-C} - \xi^{n-2N-C}}{N(1-\xi^{-1})} \\ \quad : \quad N/2 \le n < N \\ \dfrac{\xi^{N+C-n} - 1}{N(1-\xi)} + \dfrac{1-\xi^{n-2N-C}}{N(1-\xi^{-1})} \\ \quad : \quad N \le n < 3N/2 + C \end{cases}\end{aligned} \tag{33}$$

The approximate expression for (33) can be derived to be

$$\begin{aligned}\mathbf{\Phi}_{\theta\boldsymbol{u}}(n,2) &\approx 1 + \frac{\sigma_\varepsilon^2}{4}(2n - 3N - 2C) \\ &: \quad N/2 \le n < 3N/2 + C\end{aligned} \tag{34}$$

Therefore, we can write the linear form of the optimum interpolator matrix between the first and the second OFDM data symbols as follows

$$\begin{aligned}\bar{G}_{\text{opt}}(n,:) &= \mathbf{\Phi}_{\theta\boldsymbol{u}}(n,:)\mathbf{\Phi}_{\boldsymbol{uu}}^{-1} \\ &\approx [1 - \frac{\sigma_\varepsilon^2}{4}(2n-N) \;\; 1 + \frac{\sigma_\varepsilon^2}{4}(2n-3N-2C)]\mathbf{\Phi}_{\boldsymbol{uu}}^{-1} \\ &\approx \frac{1}{N+C}[-n + \frac{3N}{2} + C \;\; n - \frac{N}{2}] = \bar{G}_L(n,:)\end{aligned} \tag{35}$$

where $\bar{G}_{\text{opt}}(n,:)$ means nth row of $\bar{G}_{\text{opt}}$ and similarly for $\mathbf{\Phi}_{\theta\boldsymbol{u}}(n,:)$ and $\bar{G}_L(n,:)$.

APPENDIX III

COMPUTATION OF THE RESIDUAL PHASE NOISE VARIANCE

Since the receiver estimates the CPEs of the two consecutive OFDM symbols, there is an estimation error incurred due to the presence of noise and interference. Furthermore, connecting these two points with a straight line will produce an interpolation error since the actual underlying phase noise process is not a linear function in the index of the OFDM samples. To compute the variance of the residual phase noise vector, it is assumed that the initial CPE estimation error is uncorrelated with the interpolation error. Therefore, the MSE of the frequency-domain phase noise vector estimate can be written as

$$\begin{aligned}\sum_{q=0}^{N-1} \mathsf{E}\left[\left|\boldsymbol{\eta}_q^m\right|^2\right] &= \mathrm{Tr}\left\{\mathsf{E}\left[\left|\boldsymbol{p}^m - \widehat{\boldsymbol{p}}^m\right|^2\right]\right\} \\ &= \frac{1}{N+C}\mathrm{Tr}\left\{\mathsf{E}\left[\left|\bar{\theta} - \boldsymbol{\Phi}_{\theta\boldsymbol{u}}\boldsymbol{\Phi}_{\boldsymbol{uu}}^{-1}\boldsymbol{u}\right|^2\right]\right\} \\ &= \frac{1}{N+C}\mathrm{Tr}\left\{\mathsf{E}\left[\left|\bar{\theta} - \boldsymbol{\Phi}_{\theta\boldsymbol{u}}\boldsymbol{\Phi}_{\boldsymbol{uu}}^{-1}\boldsymbol{u}_g\right|^2\right]\right\} \\ &+ \frac{1}{N+C}\mathrm{Tr}\left\{\mathsf{E}\left[\left|\boldsymbol{\Phi}_{\theta\boldsymbol{u}}\boldsymbol{\Phi}_{\boldsymbol{uu}}^{-1}(\boldsymbol{u}_g - \boldsymbol{u})\right|^2\right]\right\}\end{aligned} \tag{36}$$

where $\boldsymbol{u}_g$ is the 2×1 vector containing the true values of CPEs and $\mathrm{Tr}\{\cdot\}$ is the trace operation. On the last line of (36), the first term on the right hand side corresponds to the interpolation error and the second term corresponds to the CPE estimation error. For small values of β, the expression for the optimum interpolator $\bar{G}_{\mathrm{opt}} = \boldsymbol{\Phi}_{\theta\boldsymbol{u}}\boldsymbol{\Phi}_{\boldsymbol{uu}}^{-1}$ can be replaced by its linear approximation $\bar{G}_L$ after which (36) is further simplified to

$$\begin{aligned}\sum_{q=0}^{N-1} \mathsf{E}\left[\left|\boldsymbol{\eta}_q^m\right|^2\right] &\approx 1 + \frac{1}{N+C}\mathrm{Tr}\left\{\bar{G}_L \boldsymbol{\Phi}_{\boldsymbol{u}_g\boldsymbol{u}_g}\bar{G}_L^T\right\} \\ &- \frac{2}{N+C}\Re\left[\mathrm{Tr}\left\{\bar{G}_L \boldsymbol{\Phi}_{\theta\boldsymbol{u}_g}^T\right\}\right] \\ &+ \frac{\sigma_{\eta_0}^2}{N+C}\mathrm{Tr}\left\{\bar{G}_L\bar{G}_L^T\right\}\end{aligned} \tag{37}$$

We assume that the auto-correlation matrix of the true CPEs equals to the auto-correlation matrix of the estimated ones i.e. $\boldsymbol{\Phi}_{\boldsymbol{u}_g\boldsymbol{u}_g} \approx \boldsymbol{\Phi}_{\boldsymbol{uu}}$ and the cross-correlation matrix of $\bar{\theta}$ and $\boldsymbol{u}_g$ is approximately equal to the cross-correlation matrix of the estimated ones i.e. $\boldsymbol{\Phi}_{\theta\boldsymbol{u}_g} \approx \boldsymbol{\Phi}_{\theta\boldsymbol{u}}$. By substituting their approximate values from (30), (32), (34) and (35) for , $\boldsymbol{\Phi}_{\boldsymbol{uu}}$, $\boldsymbol{\Phi}_{\theta\boldsymbol{u}}$ and

$\bar{G}_L$, respectively, and performing some straightforward algebra, (37) is simplified to

$$\sum_{q=0}^{N-1} \mathsf{E}\left[\left|\boldsymbol{\eta}_q^m\right|^2\right] \approx \frac{\pi\beta(N+C)T_s}{9} + \frac{2}{3}\sigma_{\eta_0}^2 \tag{38}$$

The approximation in (38) assumes large OFDM symbol size i.e $1 \ll N+C$. The performance of the CPE estimator during the data transmission stage can also be computed using (12) which takes the average of the received signal equalized by the estimated channel at $|\mathcal{P}|$ pilot positions and; therefore, the variance of the CPE estimator can be shown to be

$$\sigma_{\eta_0}^2 = \frac{1}{|\mathcal{P}|}\left(\frac{\pi\beta N T_s}{3} + \frac{1}{\bar{\gamma}}\right) \tag{39}$$

REFERENCES

[1] Y. G. Li and G. Stüber, "OFDM for wireless communications," *Springer, Inc*, January 2006.

[2] S. Wu and Y. Bar-Ness, "OFDM systems in the presence of phase noise: Consequences and solutions," *IEEE Transactions on Communications*, vol. 52, no. 11, pp. 1988–1996, November 2004.

[3] D. Petrovic, W. Rave, and G. Fettweis, "Effects of phase noise on OFDM systems with and without PLL: Characterization and compensation," *IEEE Transactions on Communications*, vol. 55, no. 8, pp. 1607–1615, August 2007.

[4] T. Pollet, M. Bladel, and M. Moeneclaey, "BER sensitivity of OFDM systems to carrier frequency offset and Wiener phase noise," *IEEE Transactions on Communications*, vol. 43, pp. 191–193, February 1995.

[5] L. Tomba, "On the effect of Wiener phase noise in OFDM systems," *IEEE Transactions on Communications*, vol. 46, pp. 580–583, May 1998.

[6] A. G. Armada and M. Calvo, "Phase noise and sub-carrier spacing effects on the performance of an OFDM communication system," *IEEE Communications Letters*, vol. 2, pp. 11–13, Jan 1998.

[7] Q. Zou, A. Tarighat, and A. H. Sayed, "Compensation of phase noise in OFDM wireless systems," *IEEE Transactions on Signal Processing*, vol. 55, no. 11, pp. 5407–5424, November 2007.

[8] S. Bittner, E. Zimmermann, and G. Fettweis, "Iterative phase noise mitigation in MIMO-OFDM systems with pilot aided channel estimation," *Vehicular Technology Conference*, September 2007.

[9] J. H. Lee, J. S. Yang, S. C. Kim, and Y. W. Park, "Joint channel estimation and phase noise suppression for OFDM systems," *Vehicular Technology Conference*, May 2005.

[10] D. D. Lin, R. A. Pacheco, T. J. Lim, and D. Hatzinakos, "Joint estimation of channel response, frequency offset, and phase noise in OFDM," *IEEE Transactions on Signal Processing*, vol. 54, no. 9, pp. 3542–3554, September 2006.

[11] P. H. Moose, "A technique for orthogonal frequency division multiplexing frequency offset correction," *IEEE Transactions on Communications*, vol. 42, pp. 2908–2914, October 1994.

[12] T. M. Schmidl and D. C. Cox, "Robust frequency and timing synchronization for OFDM," *IEEE Transactions on Communications*, vol. 45, no. 12, pp. 1613–1621, December 1997.

[13] *Part 11: Wireless LAN Medium Access Control (MAC) and Physical Layer (PHY) specifications: High-speed Physical Layer in the 5 GHz Band*, IEEE.

[14] T. C. W. Schenk, R. W. van der Hofstad, E. R. Fleddetus, and P. F. M. Smulders, "Distribution of the ICI term in phase noise impaired OFDM systems," *IEEE Transactions on Wireless Communications*, vol. 6, no. 4, pp. 1488–1500, April 2007.

[15] L. Zhao and W. Namgoong, "A novel phase noise compensation scheme for communication receivers," *IEEE Transactions on Communications*, vol. 54, no. 3, pp. 532–542, March 2006.

[16] G. J. Foschini and G. Vannucci, "Characterizing filtered light waves corrupted by phase noise," *IEEE Transactions on Information Theory*, vol. 34, no. 6, pp. 1437–1448, November 1988.

[17] A. Demir, A. Mehrotra, and J. Roychowdhury, "Phase noise in oscillators: A unifying theory and numerical methods for characterization," *IEEE Transactions on Circuits and Systems I*, vol. 47, no. 5, pp. 655–674, May 2000.

[18] S. Kay, *Fundamentals of Statistical Signal Processing*. Prentice-Hall: Upper Saddle River, 1993.

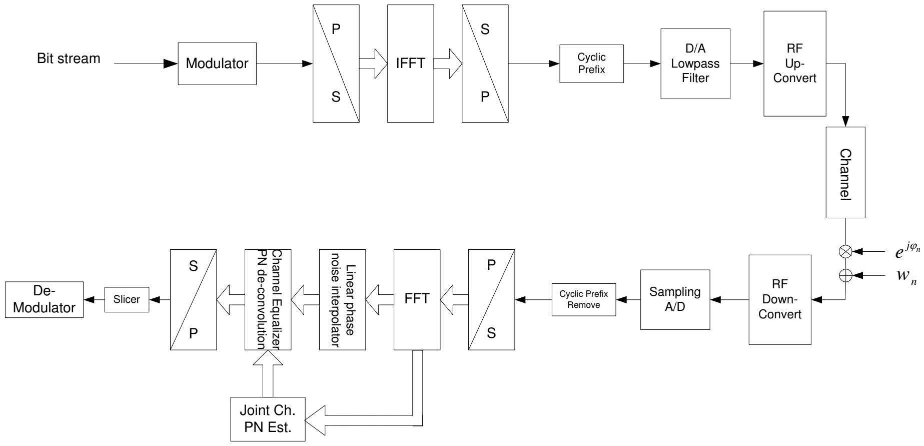

Fig. 1. Block diagram of the proposed receiver

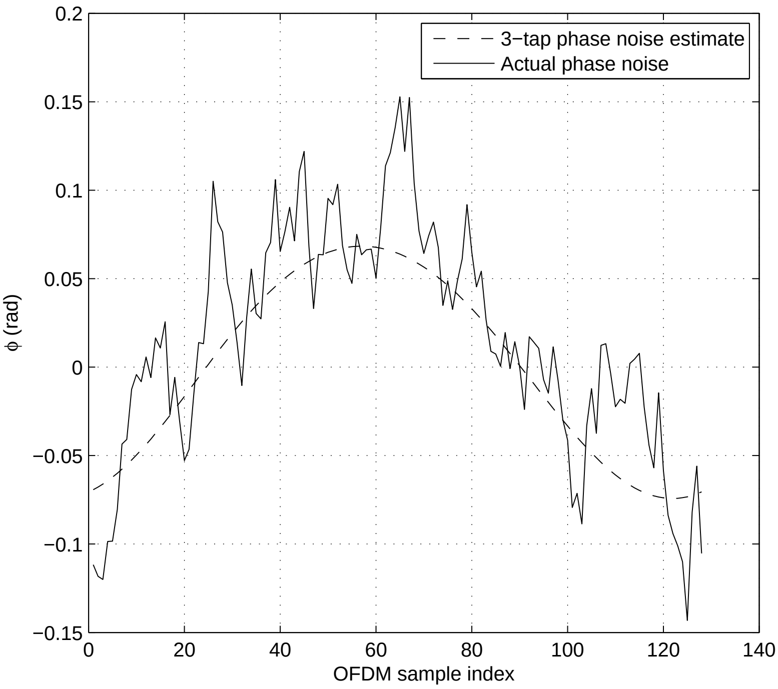

Fig. 2. Phase noise estimation during preamble transmission. 3 phase noise spectral components are estimated and $\beta = 1$kHz

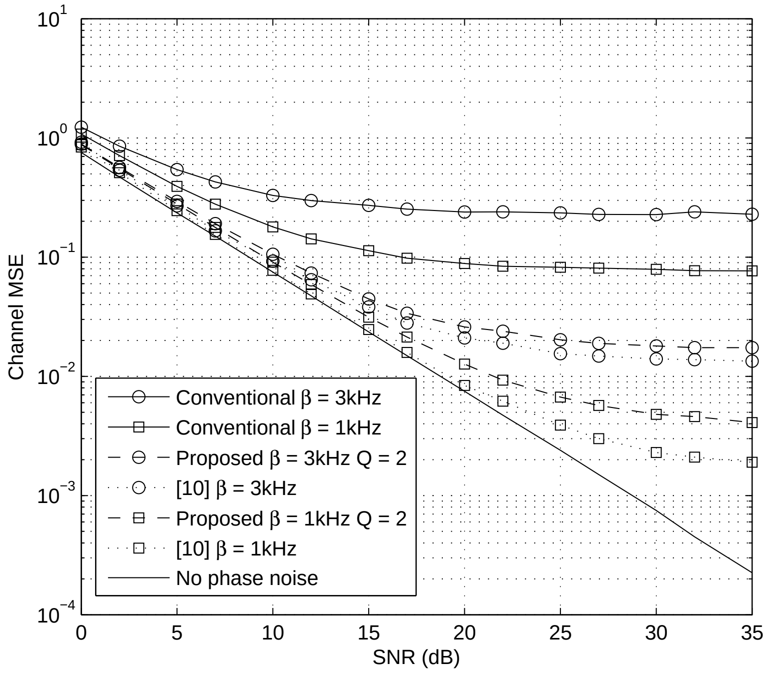

Fig. 3. Comparison of channel estimation MSE in the presence of phase noise with the scheme in [10] and the conventional case for two different values of β assuming $Q = 2$

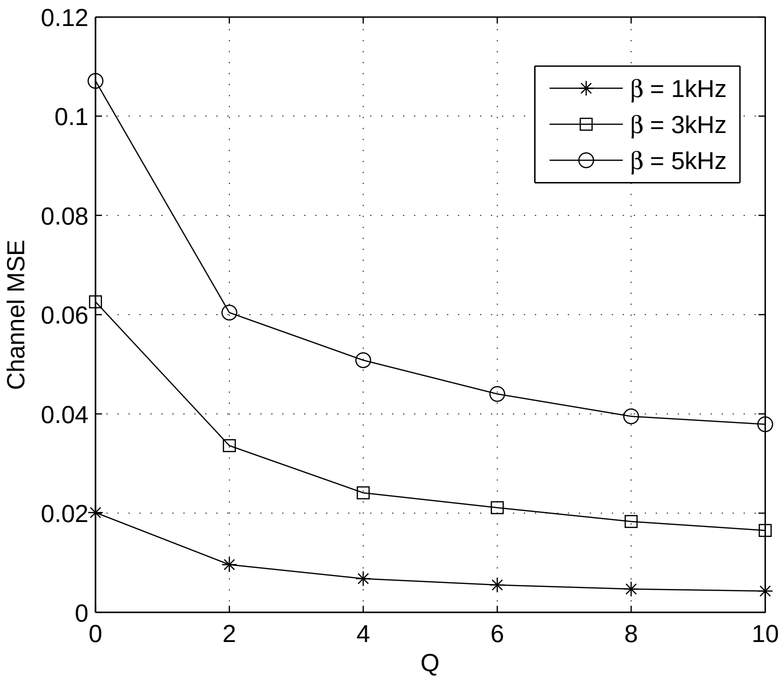

Fig. 4. Channel estimation MSE as a function of Q at SNR = 30dB

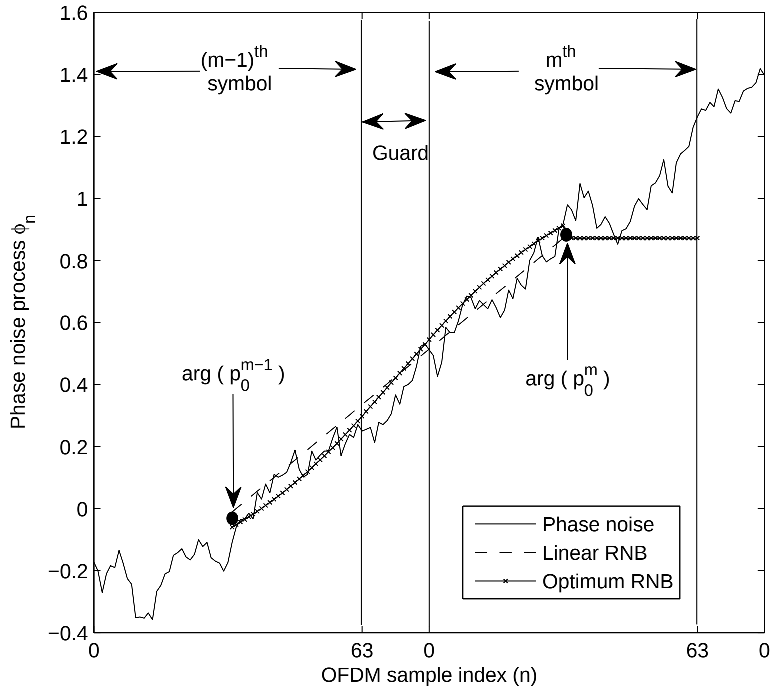

Fig. 5. RNB phase noise interpolation algorithm for $\beta = 3$kHz. The phase of the CPE of each data OFDM symbol is used to cover the second half of the interpolation region

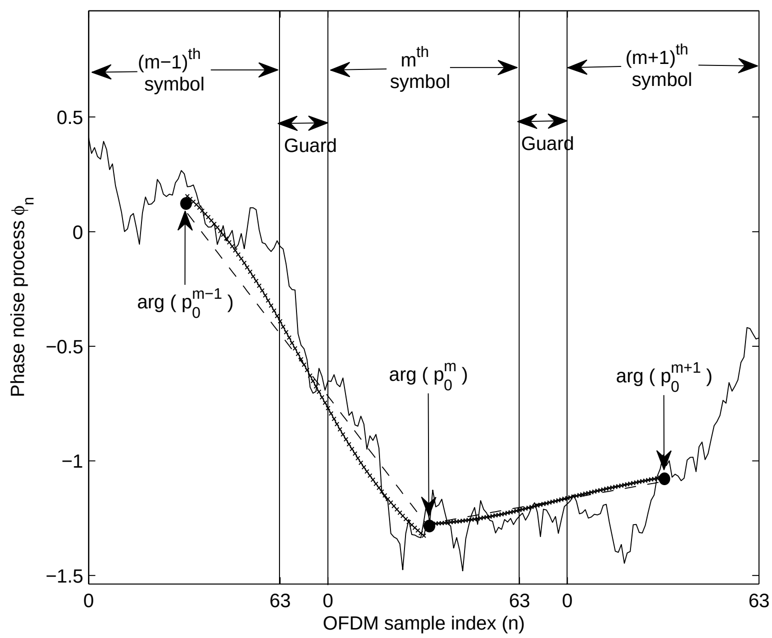

Fig. 6. RWB phase noise interpolation algorithm for $\beta = 3$kHz. The optimum and linear interpolators are shown

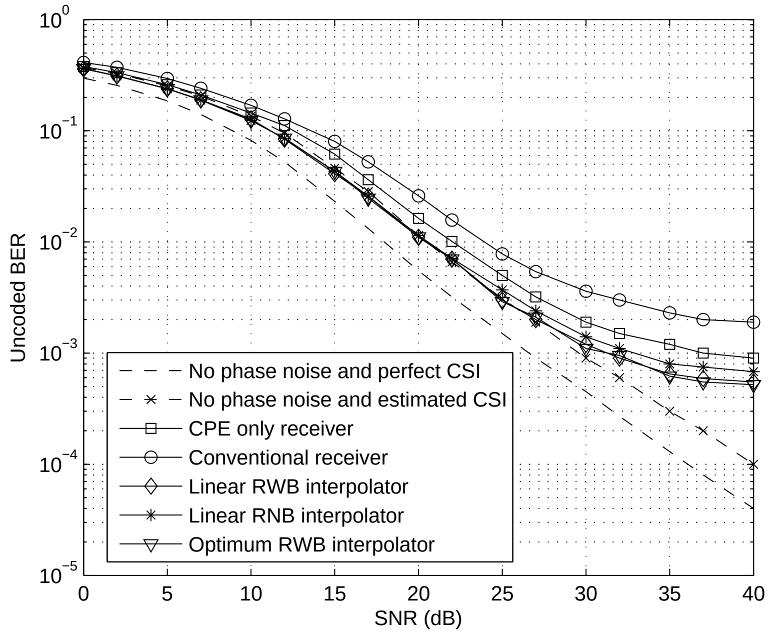

Fig. 7. Uncoded bit error rate performance of the proposed receivers with $\beta = 1$kHz and 16-QAM signal constellation

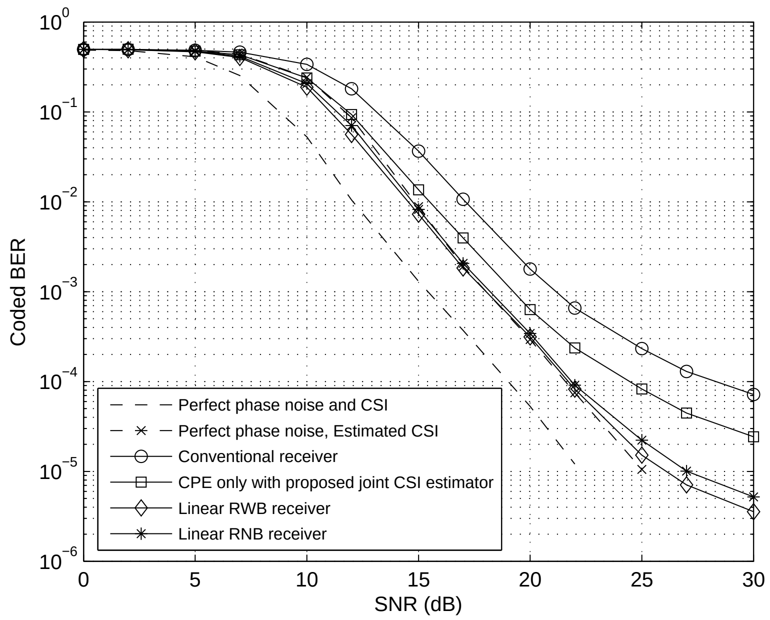

Fig. 8. Coded bit error rate performance of the proposed receivers with $\beta = 1$kHz and 16-QAM signal constellation

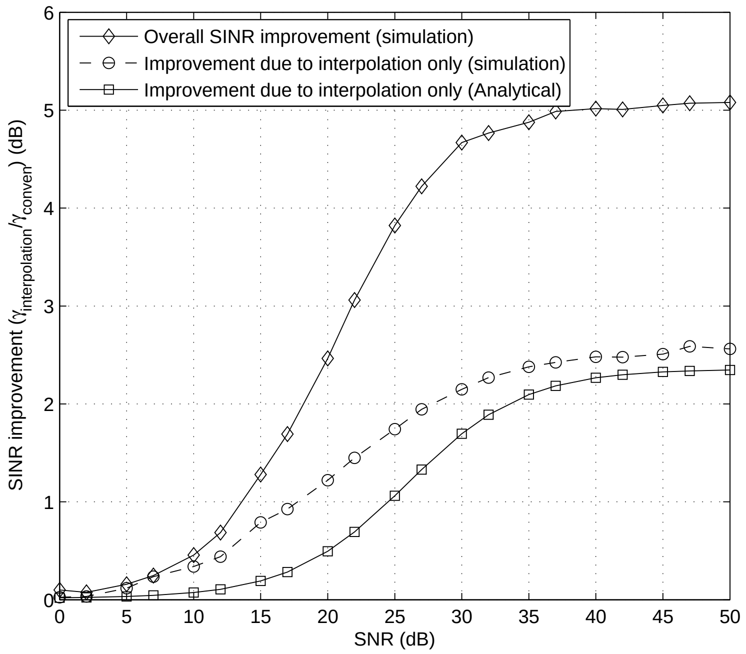

Fig. 9. SINR improvement $\bar{\gamma}_{\text{interpolation}}/\bar{\gamma}_{\text{conven}}$ versus matched filter bound SNR. $\beta = 1\text{kHz}$